Supporting Information

Calix[2]triazole[2]arene-Based Fluorescent Chemosensor for Probing the Copper Trafficking Pathway in Wilson's Disease

Jihee Cho,[†] Tuhin Pradhan,[‡] Yun Mi Lee,[†] Jong Seung Kim,[,‡] and Sanghee Kim[*,†]*

[†] College of Pharmacy, Seoul National University, Seoul 151-742, Korea

[‡] Department of Chemistry, Korea University, Seoul 136-701, Korea

Contents

1. Synthesis

General methods. All chemicals were reagent grade and were used as purchased. All reactions were performed in an inert atmosphere of dry argon or nitrogen using distilled dry solvents. Reactions were monitored by TLC analysis using silica gel 60 F-254 TLC plates. Melting points are uncorrected. Flash column chromatography was carried out on a silica gel (230–400 mesh). ^{1}H NMR (500 or 400 MHz) and ^{13}C NMR (125 or 75 MHz) spectra were recorded in δ units relative to the non-deuterated solvent as an internal reference. IR spectra were measured on a Fourier Transform Infrared spectrometer. High-resolution mass spectra (HRMS) were recorded using electron impact (EI), fast atom bombardment (FAB), or chemical ionization (CI).

Pyrenyl-appended calix[2]triazole[2]arene (2).

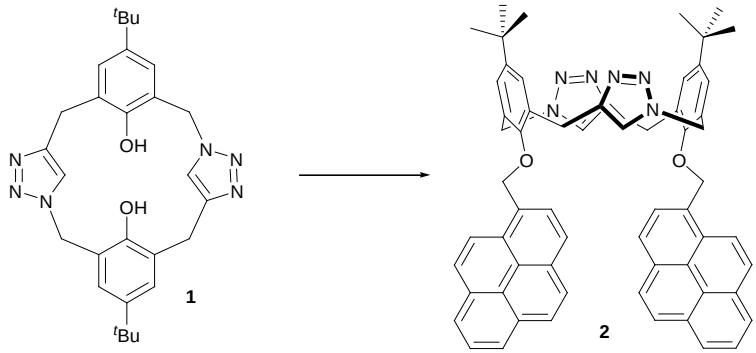

To a solution of cyclodimer **1** (50.0 mg, 0.103 mmol) in DMF (10 mL) at –40 °C was added NaH (12.0 mg, 0.500 mmol). A solution of 1-bromomethylpyrene (148 mg, 0.500 mmol) in DMF (2 mL) was added slowly to the solution and stirred for 12 h. The reaction mixture was allowed to warm to rt and neutralized with 1 N HCl. The mixture was diluted with water, and then extracted with chloroform. The organic layer was washed with water and brine, dried with $MgSO_4$, and concentrated in vacuo. The

residue was purified by column chromatography on silica gel (CH_2Cl_2/acetone, 50:1) to give **2** (93.0 mg, 99%) as a pale yellow solid: m.p 172–180 °C; ^{1}H NMR ($CDCl_3$, 500 MHz) 7.91–7.63 (m, 16H), 7.41 (d, *J* = 7.8 Hz, 2H), 7.27 (d, *J* = 2.2 Hz, 2H), 7.14 (d, *J* = 2.2 Hz, 2H), 7.05 (s, 2H), 5.40 (s, 4H), 5.37 (d, *J* = 13.9 Hz, 2H), 5.01 (d, *J* = 13.9 Hz, 2H), 4.33 (d, *J* = 15.3 Hz, 2H), 3.83 (d, *J* = 15.3 Hz, 2H), 1.20 (s, 18H) ppm.; ^{13}C NMR ($CDCl_3$, 125 MHz) 153.7 (2C), 148.3 (2C), 147.6 (2C), 133.5 (2C), 131.4 (2C), 130.9 (2C), 130.3 (2C), 129.9 (2C), 129.3 (2C), 128.8 (2C), 127.9 (2C), 127.7 (2C), 127.67 (2C), 127.6 (2C), 127.1 (2C), 126.5 (2C), 125.7 (2C), 125.2 (2C), 125.1 (2C), 124.5 (2C), 124.3 (2C), 122.2 (2C), 121.4 (2C), 74.3 (2C), 51.1 (2C), 34.4 (2C), 31.2 (6C), 31.17 (2C), 29.9 (2C) ppm.; IR ($CHCl_3$) υ_{max} 2966, 1739, 1484, 1364, 1200, 847, 755 (cm^{-1}); MS (FAB) *m/z* 915 ($[M+1]^+$, 6), 429 (2), 289 (2), 215 (100); HRMS (FAB) calcd for $C_{62}H_{55}N_6O_2$ 915.4387 ($[M+H]^+$), found 915.4373.

Pyrenyl-appended calix[4]arene.

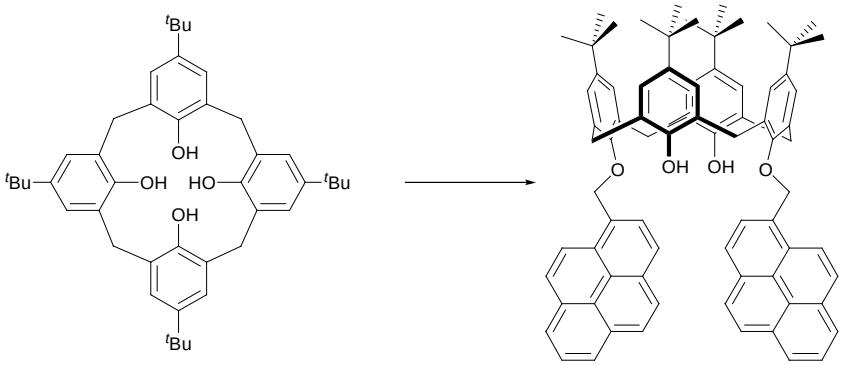

p-tert-Butylcalix[4]arene Pyrenyl-appended calix[4]arene

To a solution of *p-tert*-butylcalix[4]arene (50.0 mg, 0.077 mmol) in acetone (3 mL) were added K_2CO_3 (96.0 mg, 0.695 mmol) and 1-bromomethylpyrene (46.0 mg, 0.156 mmol). The resulting mixture was stirred under reflux for 12 h. After evaporation of the solvent, the residue was dissolved in chloroform. The organic layer was washed with 1

N HCl and brine, dried with $MgSO_4$, and concentrated in vacuo. The residue was purified by column chromatography on silica gel (hexane/EtOAc, 10:1) to give pyrenyl-appended calix[4]arene (59.0 mg, 71%) as a pale yellow solid: m.p 180–190 °C; ^{1}H NMR ($CDCl_3$, 400 MHz) 8.41–7.79 (m, 18H), 7.42 (s, 2H), 7.01 (s, 4H), 6.83 (s, 4H), 5.78 (s, 4H), 4.35 (d, *J* = 13.0 Hz, 4H), 3.24 (d, *J* = 13.1 Hz, 4H), 1.26 (s, 18H), 0.98 (s, 18H) ppm.; ^{13}C NMR ($CDCl_3$, 75 MHz) 150.8 (2C), 150.3 (2C), 147.2 (2C), 141.4 (2C), 132.8 (4C), 131.3 (2C), 131.1 (2C), 130.8 (2C), 130.3 (2C), 128.6 (2C), 127.9 (2C), 127.7 (4C), 127.6 (2C), 127.3 (2C), 126.5 (2C), 125.9 (2C), 125.6 (4C), 125.2 (4C), 125.1 (2C), 124.9 (4C), 124.8 (2C), 124.6 (2C), 123.0 (2C), 76.3 (2C), 34.0 (2C), 33.8 (2C), 31.9 (4C), 31.7 (6C), 31.0 (6C) ppm.; IR ($CHCl_3$) υ_{max} 3444, 2961, 1738, 1484, 1362, 1206, 846 (cm^{-1}); MS (FAB) *m/z* 1076 (M^+, 1), 860 (2), 611 (3), 429 (19); HRMS (FAB) calcd for $C_{78}H_{76}O_4$ 1076.5744 (M^+), found 1076.5781.

2. Theoretical studies

Calculation details. The geometry of **2**, the **2**-Cu^{2+} complex and the structure after eliminating the metal ion (Cu^{2+}) from the complex was optimized at the B3LYP/6-31G(d) level of theory. No imaginary frequencies were available after vibration analysis of the optimized structures, which indicated that each of the optimized structures was at the real minimum on the potential energy surfaces (PES). Basis set superposition errors (BSSE) were corrected by the counterpoise correction method,[1] which was applied to an optimized geometry while calculating binding energy. Binding energy (B.E) was defined by the following relationship (1), where E_{Ligand} and $E_{M^{2+}}$ were the optimized energies of ligand **2** and the metal ions (such as Cu^{2+}), respectively, and $E_{BSSEcomplex}$ indicated the counterpoise-corrected energy for the complexes.

$$B.E = E_{BSSEcomplex} - \left(E_{Ligand} + E_{M^{2+}}\right) \qquad (1)$$

All calculations were performed using the Gaussian 09 W program package.[2]

(1) S. Simon, M. Duran and J. J. Dannenberg, *J. Chem. Phys.*, 1996, **105**, 11024.
(2) M. J. Frisch et al. *Gaussian 09*, Revision B. 01, Gaussian, Inc., Wallingford, CT, 2010.

3. Time-resolved fluorescence emission studies

Experimental details. Time-resolved fluorescence emission intensity decay was analyzed using the time-correlated single photon counting (TCSPC) technique based on a picosecond pulsed diode laser system (FluoTime 200, PicoQuant GmbH, Germany) with a laser source that provided 375 nm light as excitation. The emission decay was collected at a magic angle at the excimer peak position (450 nm). As there were very low counts at the monomer emission peak at 376 or 396 nm, we could not collect decays at those peaks. From the UV-Vis spectroscopic studies (Figure S3a), we observed that a new band at 375 nm grew upon the stepwise addition of Cu^{2+}. This result may have occurred due to complexation of Cu^{2+} with **2**, enabling us to excite the complexes with 375 nm laser light. We were unable to collect the decay for only probe **2** with the available laser source because the absorption band of **2** reaches the end in the absence of Cu^{2+} (Figure S3a). The full width at the half-maximum of the instrument response function (IRF) with the above excitation was approximately 200 ps. The collected emission decays were deconvoluted from the IRF and fitted to a multiexponential function using an iterative reconvolution algorithm.[3] All experiments were performed at room temperature.

(3) (a) K. Dahl, R. Biswas, N. Ito and M. Maroncelli, *J. Phys. Chem. B,* 2005, **109**, 1563. (b) T. Pradhan and R. Biswas, *J. Phys. Chem. A*, 2007, **111**, 11524. (c) T. Pradhan, P. Ghoshal and R. Biswas, *J. Phys. Chem. A,* 2008, **112**, 915. (d) R. Biswas, N. Rohman, T. Pradhan and R. Buchner, *J. Phys. Chem. B,* 2008, **112**, 9379. (e) T. Pradhan, H. A. R. Gazi and R. Biswas, *J. Chem. Phys.*, 2009, **131**, 054507.

Table S1. Fit parameters for the excimer emission decays in $Cu(ClO_4)_2$ solutions of acetonitrile.

Conc. of Cu^{2+} (μM)	$\tau_1(ns)$	$\tau_2(ns)$	a_1	a_2	χ^2
45	24.59	2.74	0.52	0.48	0.918
182	24.62	2.43	0.49	0.51	0.905
305	24.10	2.41	0.52	0.48	0.916
519	24.06	2.42	0.52	0.48	0.864
750	23.99	2.42	0.51	0.49	0.906
1530	23.87	2.44	0.53	0.47	0.924

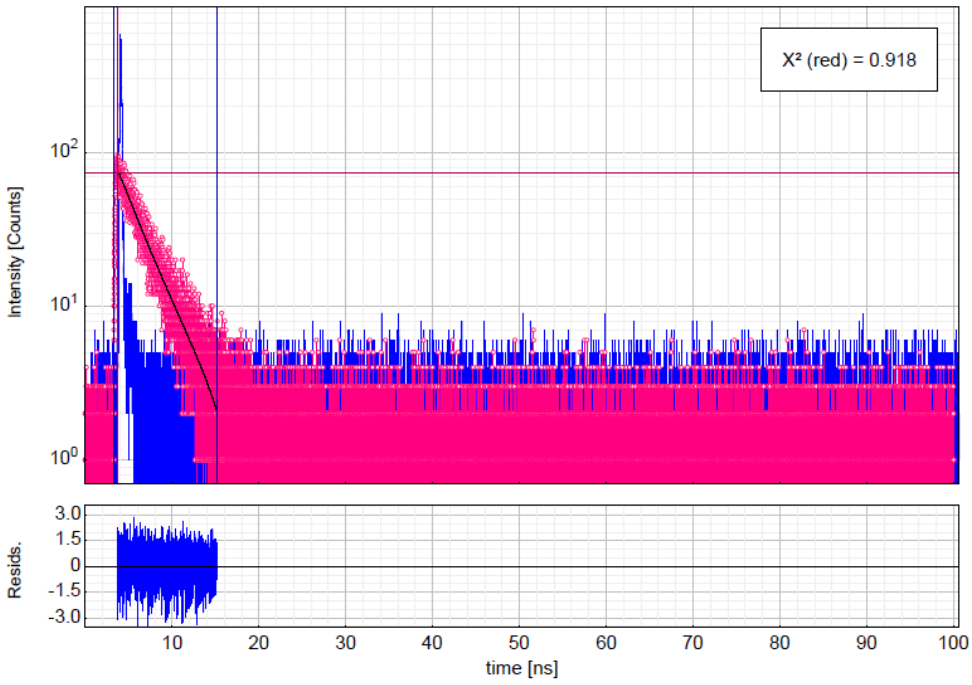

Figure S1. A representative excimer emission decay of **2** in a $Cu(ClO_4)_2$ solution of acetonitrile (45 μM) is shown in this figure. The data are represented by the circles (red), the fit to the data is represented by the solid line (black) and the instrument response function (irf) is shown by line plots (blue). The fit (biexponential) results are provided in Table S1. Residuals are shown at the bottom of the panel (blue color, ± 3 full scale). The concentration of **2** in solution was ~ 10 μM.

4. Absorption and fluorescence spectra

General methods. All UV/Vis absorption and fluorescence spectra were recorded using a HITACHI JP/U-3010 and a JASCO FP-6500 instrument, respectively. All reagents and cationic compounds, such as $Zn(ClO_4)_2 \cdot 6H_2O$, $Pb(ClO_4)_2 \cdot xH_2O$, $Ba(ClO_4)_2$, $Ca(ClO_4)_2 \cdot 4H_2O$, $Cd(ClO_4)_2 \cdot H_2O$, $NaClO_4$, $Mg(ClO_4)_2$, $AgClO_4$, $Sr(ClO_4)_2 \cdot H_2O$, $Mn(ClO_4)_2 \cdot xH_2O$, $LiClO_4$, $Cu(ClO_4)_2 \cdot 6H_2O$, $Co(ClO_4)_2 \cdot 6H_2O$, $Cr(ClO_4)_3 \cdot 6H_2O$, $Hg(ClO_4)_2 \cdot H_2O$, $In(ClO_4)_3 \cdot H_2O$, $Al(ClO_4)_3 \cdot 9H_2O$, $Ni(ClO_4)_2 \cdot 6H_2O$ and $[(MeCN)_4Cu]PF_6$ were purchased from Sigma-Aldrich. All solvents were analytical grade. The acetonitrile used for the collection of spectra was HPLC grade without fluorescent impurities. Stock solutions (10 mM) of metal perchlorates were prepared in acetonitrile. Stock solutions (60 μM) of **2** and pyrenyl-appended calix[4]arene were prepared in acetonitrile. Excitation was carried out at 344 nm with 3 nm excitation and emission slit widths. Titration experiments were performed with 6 μM solutions of **2** in acetonitrile and various concentrations of $Cu(ClO_4)_2$.

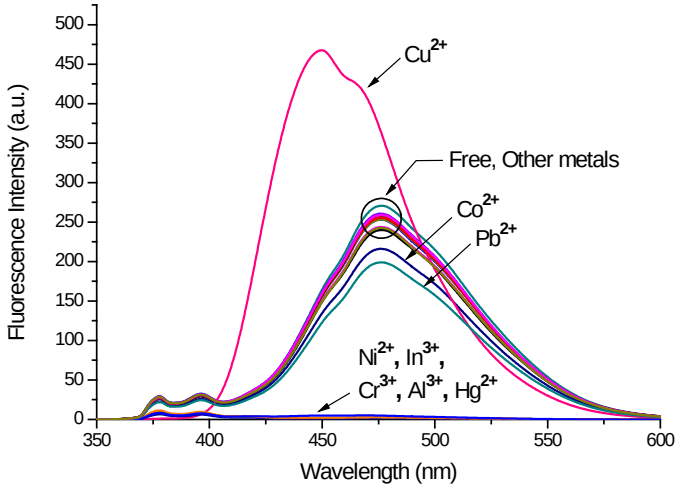

Figure S2. Fluorescence spectra of **2** (6 μM) in acetonitrile and in the presence of 100 equiv of Zn^{2+}, Pb^{2+}, Cu^{+}, Ba^{2+}, Ca^{2+}, Cd^{2+}, Na^{+}, Mg^{2+}, Ag^{+}, Sr^{2+}, Mn^{2+}, Li^{+}, Cu^{2+}, Co^{2+}, Cr^{3+}, Hg^{2+}, In^{3+}, Al^{3+} or Ni^{2+} (excitation at 344 nm).

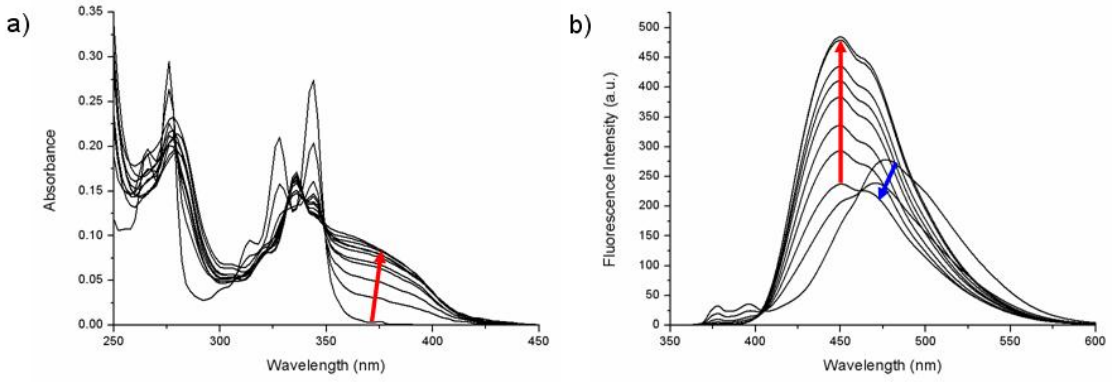

Figure S3. (a) Absorption spectra and (b) emission spectra of **2** (6 μM) upon titration with $Cu(ClO_4)_2$ (0, 1, 2, 4, 6, 10, 30, 50, 80, 100 or 120 equiv) in acetonitrile.

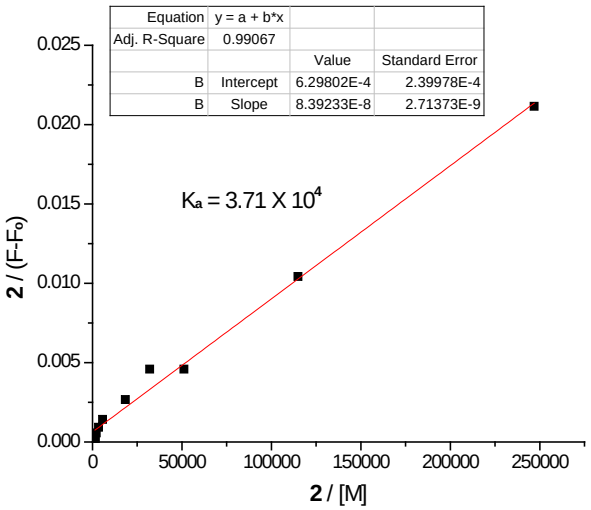

Figure S4. Benesi-Hildebrand plot of **2** with Cu^{2+} in acetonitrile.

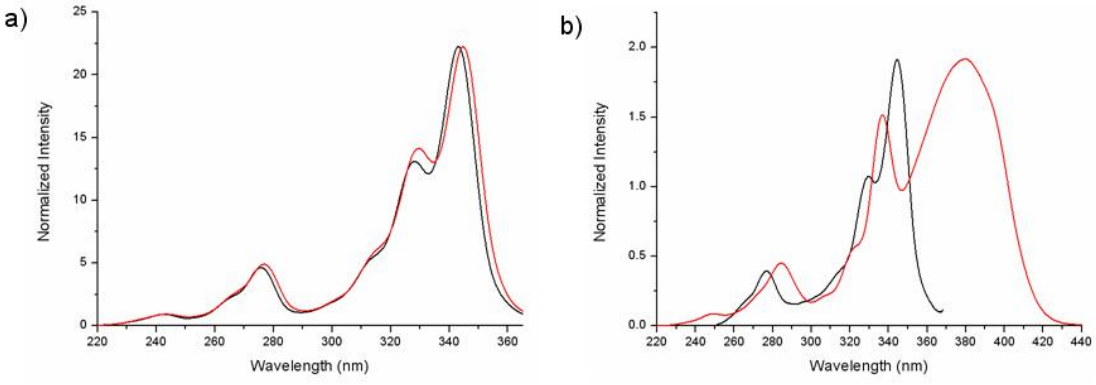

Figure S5. (a) Excitation spectra (normalized) of free **2** monitored at 377 nm (black) and 476 nm (red). (b) Excitation spectra (normalized) of **2** monitored at 377 nm (black) and 450 nm (red) in the presence of 100 equiv of $Cu(ClO_4)_2$.

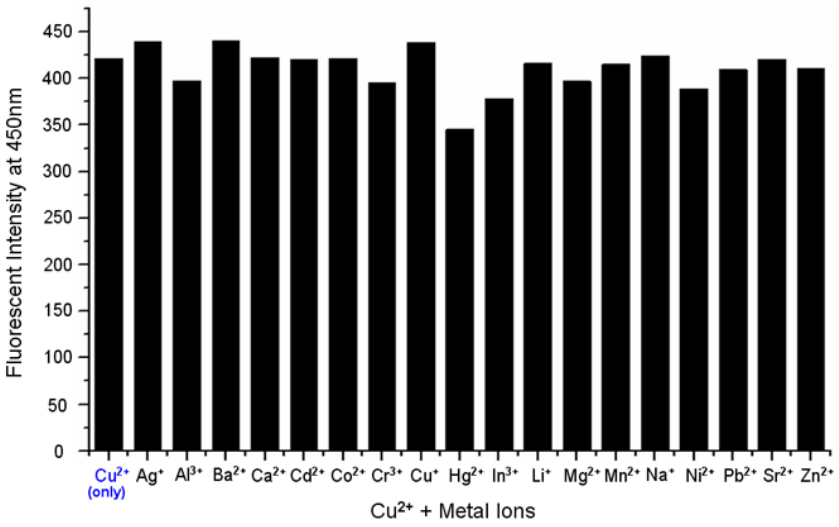

Figure S6. Fluorescence response at 450 nm of **2** (6 μM) containing 50 equiv of $Cu(ClO_4)_2$ to the selected metal ions (50 equiv) in acetonitrile.

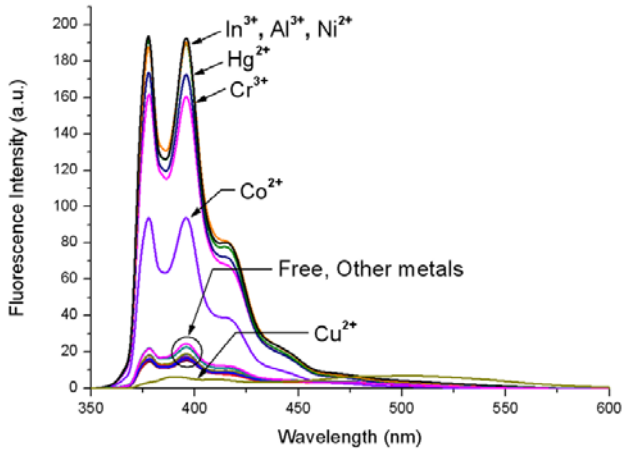

Figure S7. Fluorescence spectra of pyrenyl-appended calix[4]arene (6 μM) in acetonitrile and in the presence of 100 equiv of Zn^{2+}, Pb^{2+}, Cu^{+}, Ba^{2+}, Ca^{2+}, Cd^{2+}, Na^{+}, Mg^{2+}, Ag^{+}, Sr^{2+}, Mn^{2+}, Li^{+}, Cu^{2+}, Co^{2+}, Cr^{3+}, Hg^{2+}, In^{3+}, Al^{3+} or Ni^{2+} (excitation at 342 nm).

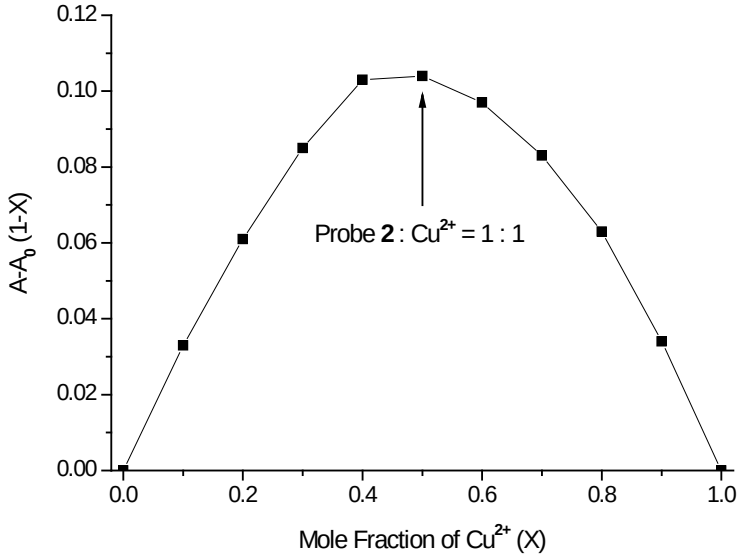

Figure S8. Job's plot of the complexation between **2** and Cu^{2+}, total concentration of **2** and Cu^{2+} was kept constant at 10 μM in acetonitrile.

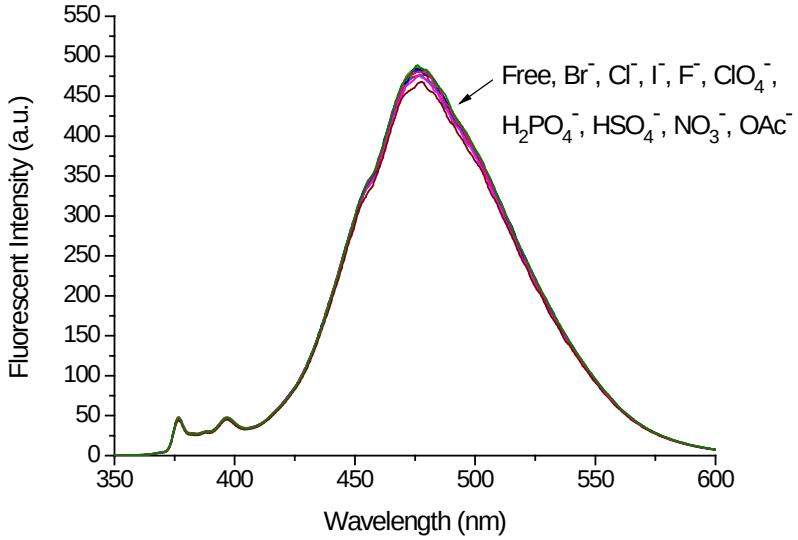

Figure S9. Fluorescence spectra of **2** (6 μM) in acetonitrile and in the presence of 100 equiv of Br^-, Cl^-, I^-, F^-, ClO_4^-, $H_2PO_4^-$, HSO_4^-, NO_3^- or OAc^- (excitation at 344 nm).

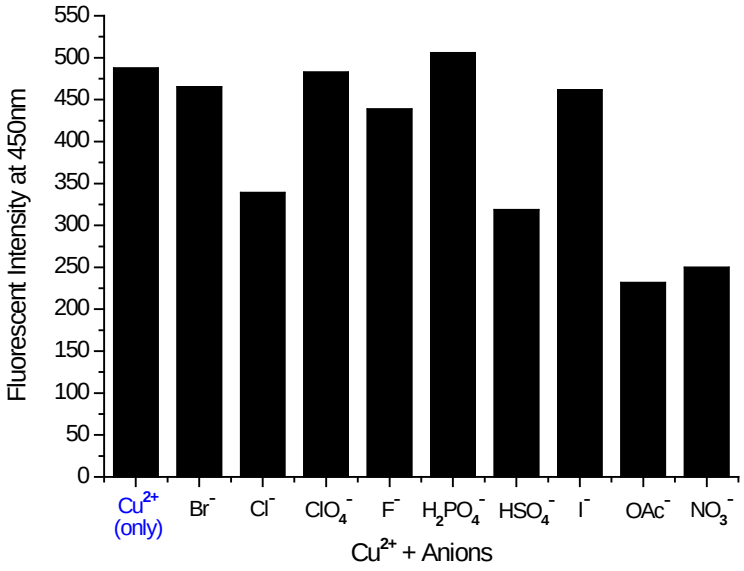

Figure S10. Fluorescence response at 450 nm of **2** (6 μM) containing 50 equiv of $Cu(ClO_4)_2$ to the selected anions (50 equiv) in acetonitrile.

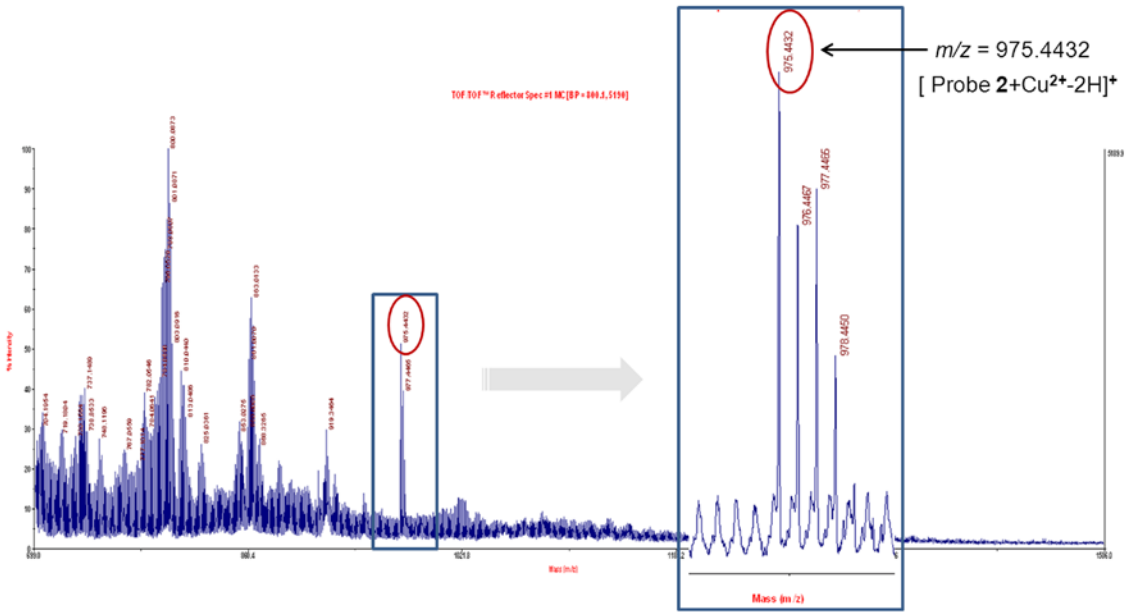

Figure S11. MALDI-TOF MS spectrum of **2**-Cu^{2+} complex in acetonitrile.

5. Cell incubation and imaging

Cell culture and reagents. Human hepatoma (HepG2) cells were provided by the Korean Cell Line Bank (KCLB). The cells were grown in MEM Alpha Modification medium (HyClone) supplemented with 10% fetal bovine serum (FBS, Invitrogen) and 1% penicillin-streptomycin (Invitrogen). All of the cell lines were incubated at 37 °C under 5% CO_2 in a humidified atmosphere and subcultured once or twice per week. ER Tracker Red (BODIPY TR glibenclamide), Golgi Tracker Red (BODIPY TR Ceramide complexed to BSA), Mito Tracker Red, Lyso Tracker Red DND-99 and propidium iodide (PI) were purchased from Invitrogen.

Fluorescence microscopy analysis. HepG2 cells were seeded onto 24-well plates and stabilized overnight. The cells were incubated with $CuCl_2$ (200 μM) prior to treatment with probe **2**. The cells were washed with PBS and then treated with probe **2** (10 μM). After incubation, residual quantities of probe **2** not taken up into the cells were removed by washing the cells with PBS. After treatment with probe **2**, the cells were incubated with ER Tracker Red (0.1 μM), Golgi Tracker Red (0.1 μM), Mito Tracker Red (1 μM) or Lyso Tracker Red DND-99 (0.1 μM) followed by washing with PBS before the cells were placed on media. Fluorescence images were taken using a fluorescence microscope (Nikon eclipse T*i*-U, 40×objective lens). Images were recorded at an excitation wavelength of 340±13 nm and an emission wavelength of 434±9 nm for blue fluorescence or 525±10 nm for green fluorescence.

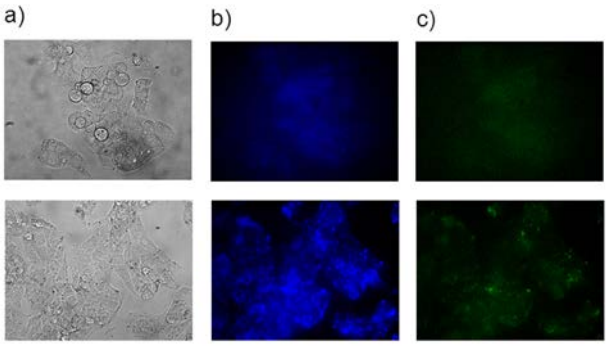

Figure S12. Fluorescence images of **2** in HepG2 cells. HepG2 cells incubated with **2** (10 μM) for 1.5 h at 37 °C (top). HepG2 cells incubated with $CuCl_2$ (200 μM) for 1 h, washed three times, and then incubated with **2** (10 μM) for 1.5 h at 37 °C (bottom). (a) Bright-field transmission images. (b) Fluorescence images in the blue region of the spectrum (λ_{ex}=340±13 nm, λ_{em}=434±9 nm). (c) Fluorescence images in the green region of the spectrum (λ_{ex}=340±13 nm, λ_{em}=525±10 nm).

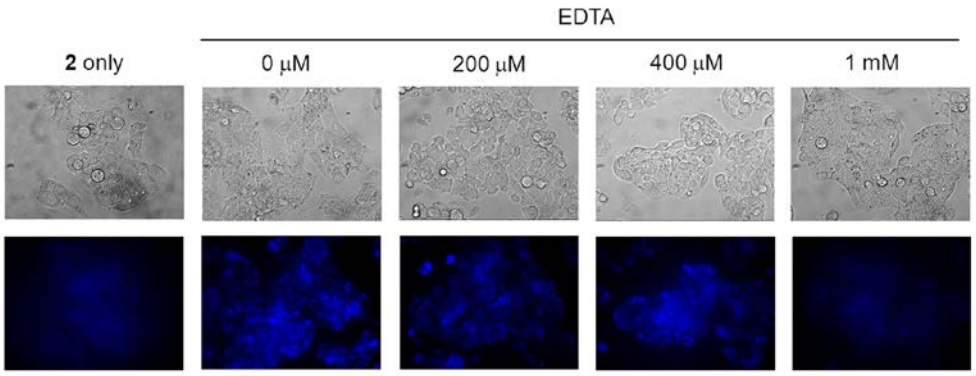

Figure S13. Fluorescence intensity changes of **2** in HepG2 cells. Bright-field transmission images (top). **2** (10 μM) + $CuCl_2$ (200 μM) pre-treated HepG2 cells incubated with different concentrations of EDTA (0, 200, 400 μM or 1 mM) for 0.5 h. Fluorescence images in the blue region of the spectrum (λ_{ex}=340±13 nm, λ_{em}=434±9 nm) (bottom).

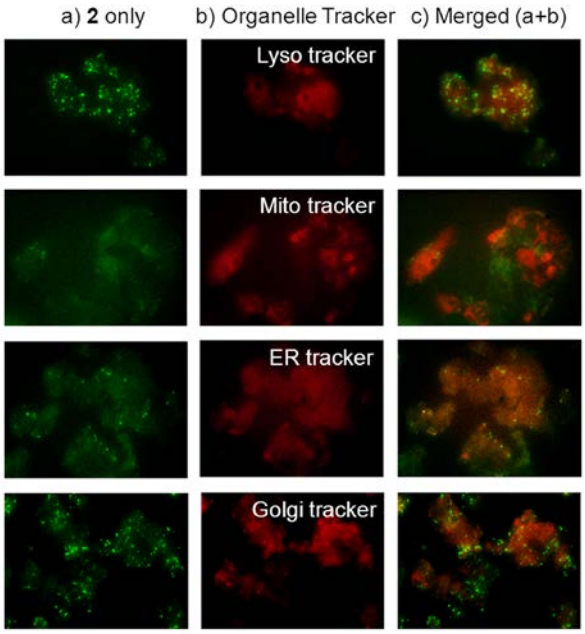

Figure S14. Localization studies of **2** in HepG2 cells. HepG2 cells incubated with **2** (10 μM) for 1.5 h and four organelle trackers (Lyso Tracker Red DND-99 (0.1 μM), Mito Tracker Red (1 μM), ER Tracker Red (0.1 μM) or Golgi Tracker Red (0.1 μM)) for 0.5 h at 37 ^{o}C. The three images in each row show the following samples: (a) Fluorescence images of cells were visualized by green emission of **2** (λ_{ex}=340±13 nm, λ_{em}=525±10 nm). (b) Fluorescence images were visualized by red emission of organelle trackers (λ_{ex}=543±22 nm, λ_{em}=593±40 nm). (c) Merged images between (a) and (b). The orange regions represent the colocalization of **2** with organelle trackers.

Additional explanation for Figure S15. For the subcellular copper localization studies, HepG2 cells were incubated with $CuCl_2$ (200 μM) for 1 h followed by treatment with probe **2** (10 μM) for 1.5 h. The lysosome, mitochondria, endoplasmic reticulum (ER), and Golgi were labeled with Lyso Tracker Red DND-99, Mito Tracker Red, ER Tracker Red, and Golgi Tracker Red, respectively. For quantitative colocalization analysis, Pearson's coefficients were calculated using the fluorescence images. The coefficient value (*r*) of the lysosome was the highest; the *r* values for the colocalization of **2** with lysosome, mitochondria, endoplasmic reticulum (ER), and Golgi apparatus are 0.93, 0.64, 0.81 and 0.73 (panels A-(c), B-(c), C-(c) and D-(c)), respectively. This analysis confirmed the literature reports that the lysosome is the major site at which copper accumulates.

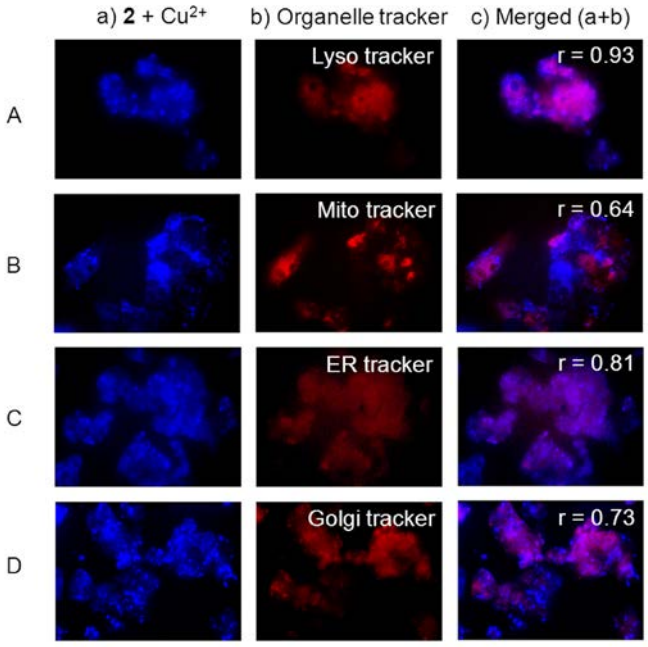

Figure S15. Localization studies of **2** in HepG2 cells. HepG2 cells incubated with $CuCl_2$ (200 μM) for 1 h, **2** (10 μM) for 1.5 h, and four organelle trackers (Lyso Tracker Red DND-99 (0.1 μM), Mito Tracker Red (1 μM), ER Tracker Red (0.1 μM) or Golgi

Tracker Red (0.1 μM)) for 0.5 h at 37 ^{o}C. The three images in each row show the following samples: (a) Fluorescence images of cells were visualized by blue emission of **2** + Cu^{2+} (λ_{ex}=340±13 nm, λ_{em}=434±9 nm). (b) Fluorescence images were visualized by red emission of organelle trackers (λ_{ex}=543±22 nm, λ_{em}=593±40 nm). (c) Merged images between (a) and (b). The violet regions represent the colocalization of **2** with organelle trackers. The degree of overlap of blue and red signal is presented as the Pearson's correlation coefficient (*r*).

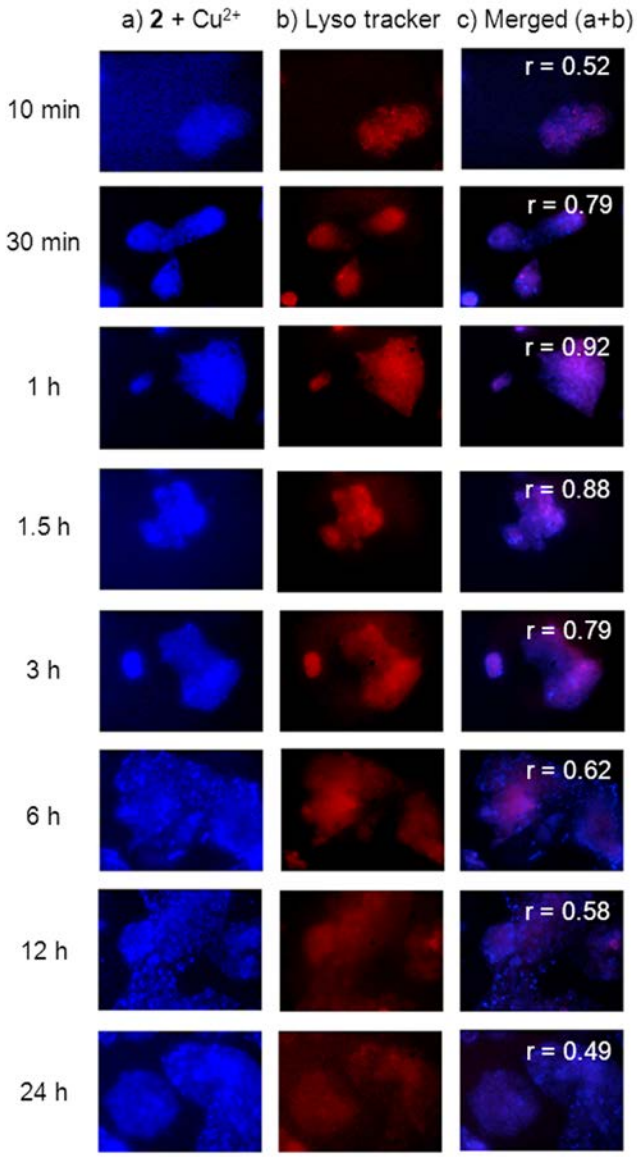

Figure S16. Localization studies of **2** in copper-induced apoptotic HepG2 cells. HepG2 cells incubated with $CuCl_2$ (200 μM) at different time periods (0 min–24 h), **2** (10 μM) for 1.5 h, and Lyso Tracker Red DND-99 (0.1 μM) for 0.5 h at 37 ^{o}C. The three images in each row show the following samples: (a) Fluorescence images of cells were visualized by blue emission of **2** + Cu^{2+} (λ_{ex}=340±13 nm, λ_{em}=434±9 nm). (b) Fluorescence images were visualized by red emission of lyso tracker (λ_{ex}=543±22 nm, λ_{em}=593±40 nm). (c) Merged images between (a) and (b). The violet regions represent the colocalization of **2** with Lyso tracker. The degree of overlap of blue and red signal is presented as the Pearson's correlation coefficient (*r*).

Propidium iodide (PI) staining. HepG2 cells were seeded onto 24-well plates and stabilized overnight. The cells were incubated with $CuCl_2$ (0, 200, 400 μM or 1 mM) for various times (6, 12, 24 or 48 h) prior to treatment with PI. The cells were washed with PBS and then treated with PI (10 μM). After incubation, residual PI was removed by washing the cells with PBS before the cells were placed on media. Fluorescence images were taken using a fluorescence microscope (Nikon eclipse T*i*-U, 40×objective lens). The fluorescence images were visualized by red emission of PI (λ_{ex}=543±22 nm, λ_{em}=593±40 nm).

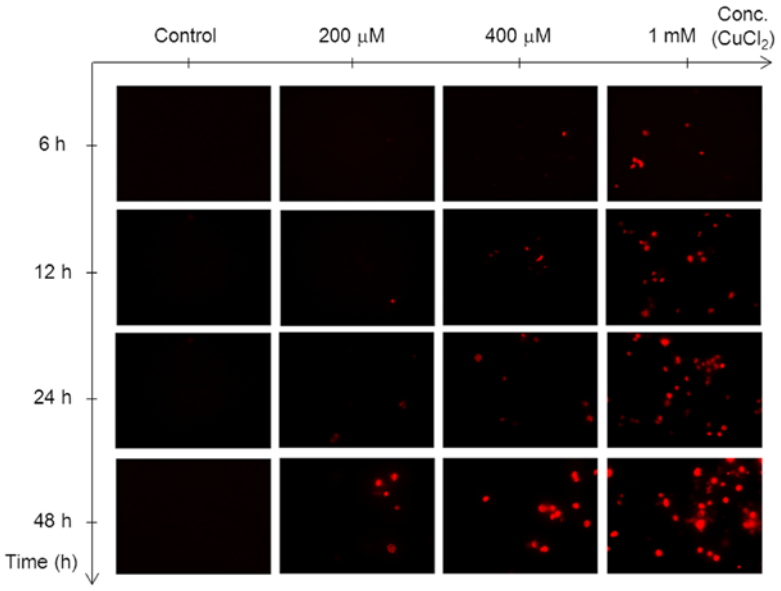

Figure S17. Effects of Cu^{2+}-induced apoptotic cell death in HepG2 cells using the PI staining assay. Cells were treated with $CuCl_2$ (0, 200, 400 μM or 1 mM) for defined periods of time (6, 12, 24 or 48 h) at 37 ^{o}C. Fluorescence images were visualized by the red emission of PI (λ_{ex}=543±22 nm, λ_{em}=593±40 nm).

6. Sulforhodamine B (SRB) assay

The cytotoxicity of the individual compounds screened was determined by the SRB assay. Briefly, cells were plated in 96-well plates at a density of 5×10^4 cells/well (HepG2) and incubated for 24 h. Test compounds (dissolved in pure DMSO) were diluted in the medium and the cells were treated for 48 h. The tested cells were then fixed with 10% trichloroacetic acid for 1 h at 4 °C. The fixed cells were stained with 0.4% sulforhodamine B (SRB) for 1 h at room temperature. The stained cells were then dissolved in 10 mM Tris (pH 10.0). The absorbance was measured at 515 nm. The cell survival (%) of each tested group was determined by comparison with solvent-treated control cells.

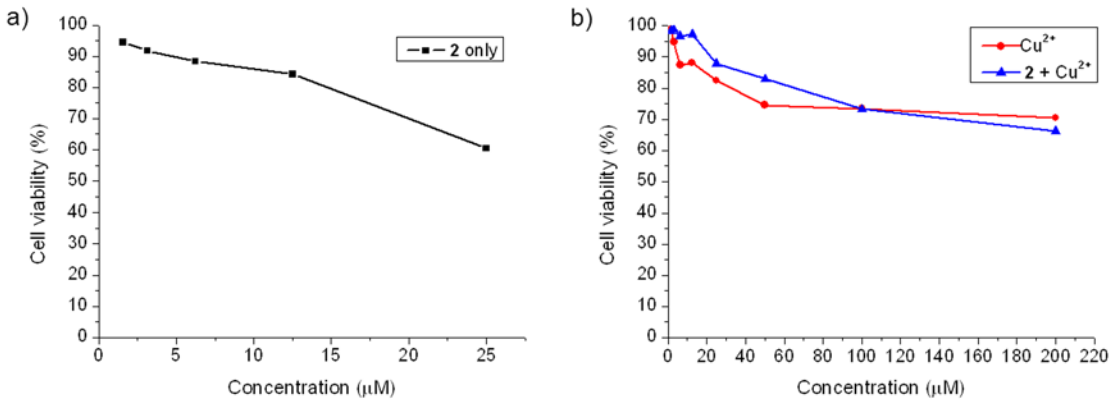

Figure S18. Percentage of HepG2 cell viability remaining after cell treatment with (a) **2**, (b) Cu^{2+} and **2** in the presence Cu^{2+} (untreated cells were considered to have 100% survival). Cell viability was assayed by the SRB method.

7. ^{1}H NMR and ^{13}C NMR spectra

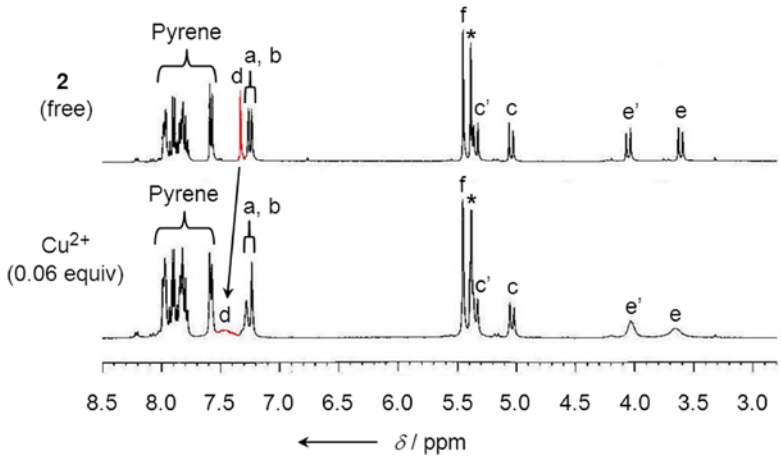

Figure S19. ^{1}H NMR spectrum of **2** in CD_3CN/CD_2Cl_2 (7:1) and its ^{1}H NMR spectrum in the presence of $Cu(ClO_4)_2$ (0.06 equiv), where * denotes the residual proton signal from CD_2Cl_2.

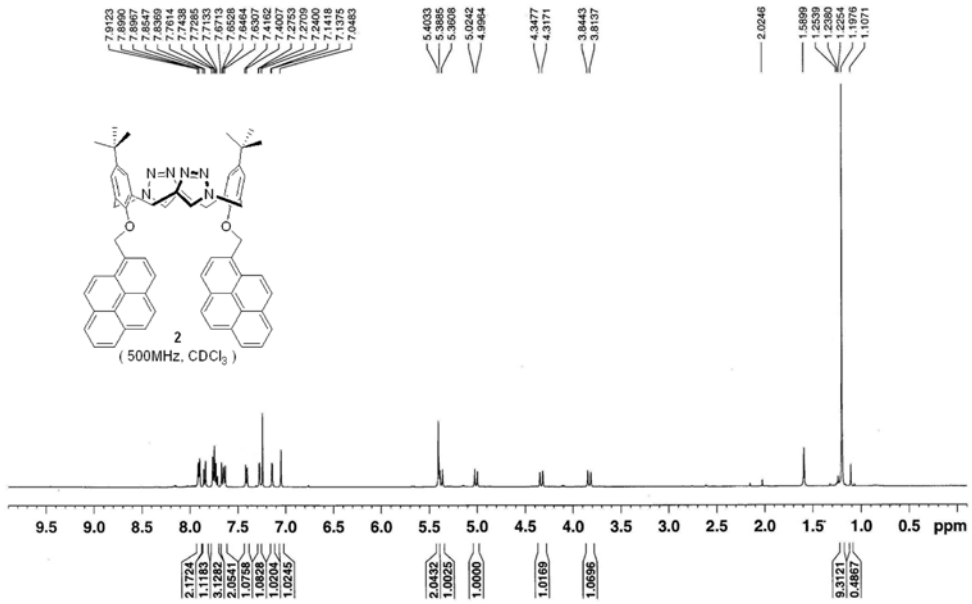

Figure S20. ^{1}H NMR spectrum of compound **2**.

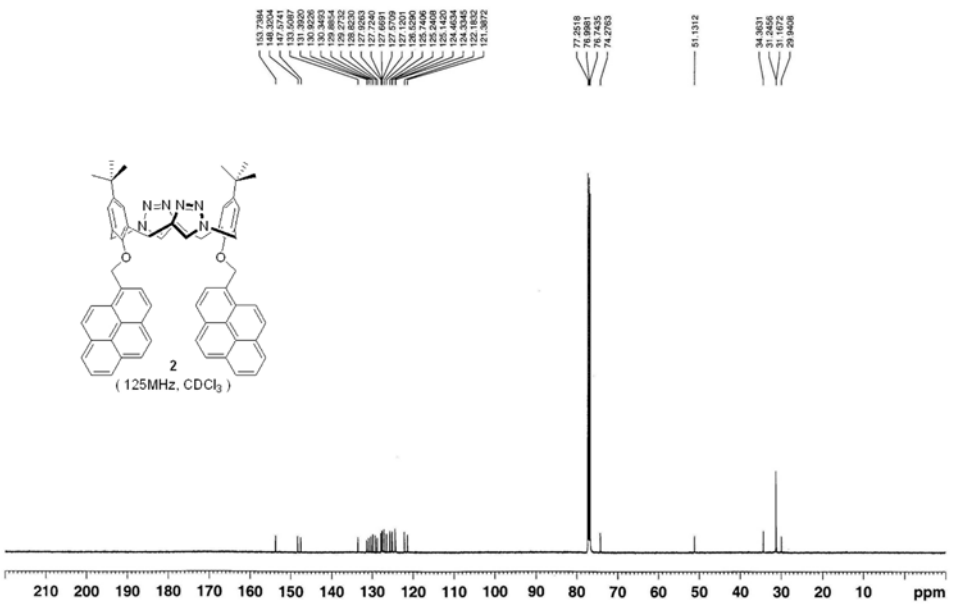

Figure S21. ^{13}C NMR spectrum of compound **2**.

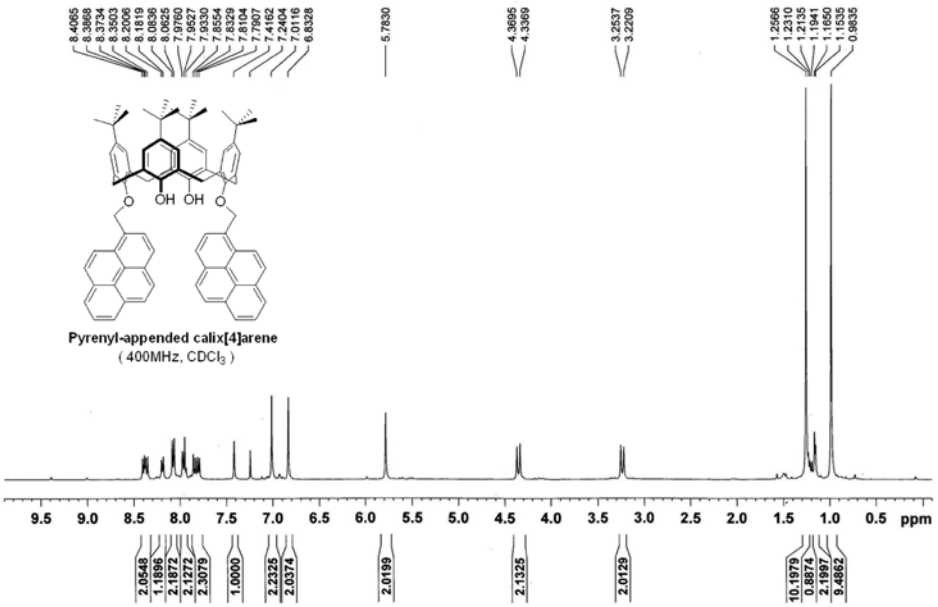

Figure S22. ^{1}H NMR spectrum of pyrenyl-appended calix[4]arene.

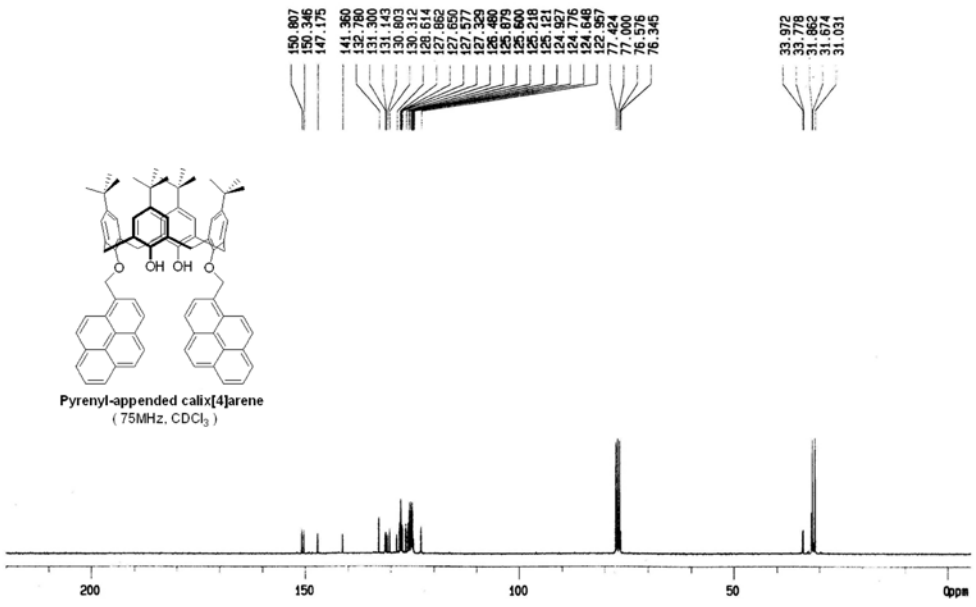

Figure S23. ^{13}C NMR spectrum of pyrenyl-appended calix[4]arene.

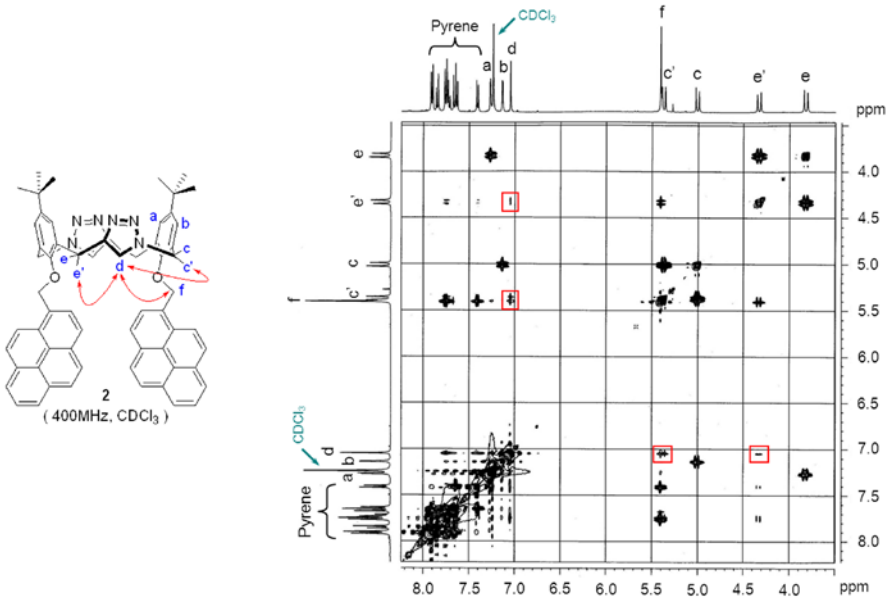

Figure S24. ^{1}H-^{1}H NOESY NMR spectrum of compound **2**.

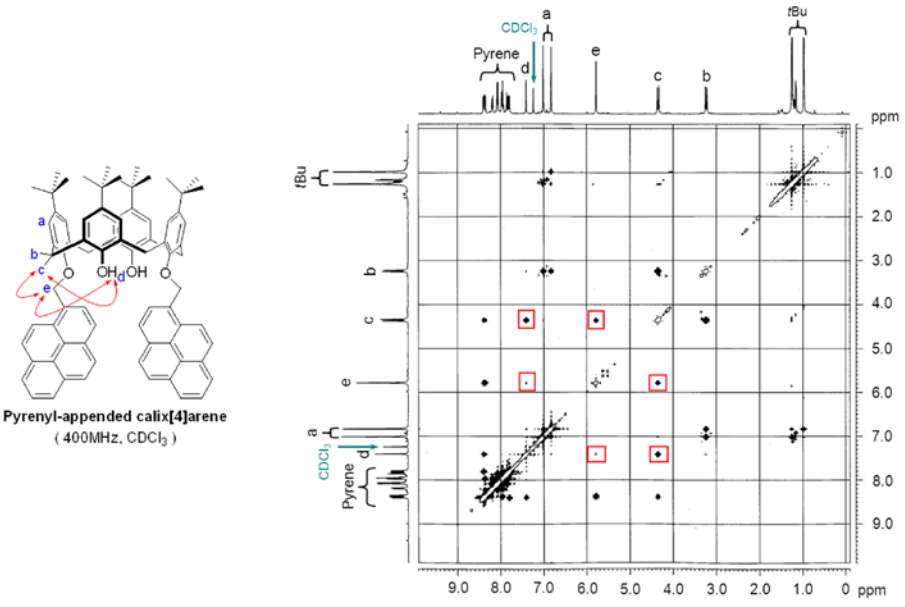

Figure S25. ^{1}H-^{1}H NOESY NMR spectrum of pyrenyl-appended calix[4]arene.